



IJVR

ISSN: 1728-1997 (Print) ISSN: 2252-0589 (Online)

Vol. 26

No.2

Ser. No. 91

2025

IRANIAN JOURNAL OF VETERINARY RESEARCH



Original Article

Investigating the effect of rosmarinic acid loaded magnetic nanoparticles against growth and biofilm formation of *Staphylococcus aureus* isolated from poultry meat

Poursafar, A.1; Asadpour, L.2* and Mokhtary, M.3

¹MSc Student in Microbiology, Department of Biology, Faculty of Basic Sciences, Rasht Branch, Islamic Azad University, Rasht, Iran; ²Department of Biology, Faculty of Basic Sciences, Rasht Branch, Islamic Azad University, Rasht, Iran; ³Department of Chemistry, Faculty of Basic Sciences, Rasht Branch, Islamic Azad University, Rasht, Iran

*Correspondence: L. Asadpour, Department of Biology, Faculty of Basic Sciences, Rasht Branch, Islamic Azad University, Rasht, Iran. E-mail: le.asadpour@iau.ac.ir



[©] 10.22099/ijvr.2025.51467.7647

(Received 20 Oct 2024; revised version 10 Apr 2025; accepted 28 Apr 2025)

This is an open access article under the CC BY-NC-ND license (http://creativecommons.org/licenses/by-nc-nd/4.0/)

Abstract

Background: Staphylococcus aureus, one of the causes of food poisoning, plays an important role in causing gastrointestinal inflammation. Aims: Given the spread of antibiotic resistance in S. aureus, the present study aimed to investigate the effect of rosmarinic acid (RA) loaded magnetic nanoparticles (Fe₃O₄NPs@RA) on inhibiting the growth and biofilm formation of S. aureus isolated from meat samples. Methods: Fe₃O₄NPs@RA have been synthesized and their antimicrobial activities were investigated against S. aureus isolated from poultry meat by broth micro-dilution. The anti-biofilm effect of these nanoparticles and their effect on the expression level of biofilm-associated genes were investigated using microplate and real-time PCR methods. The killing properties of Fe₃O₄NPs@RA against test bacteria investigated by time-kill assay. Results: The minimum inhibitory concentration (MIC) of Fe₃O₄NPs@RA against S. aureus isolates ranged from 31.2-125 μg/ml. Also, the treatment with a sub-MIC concentration of Fe₃O₄NPs@RA prevented the formation of biofilm by 50-82%, in different isolates and downregulated the expression level of icaA and icaD. Also, the treatment with the MIC concentration of Fe₃O₄NPs@RA caused a 2.4-fold decrease in the population of living bacteria after 4 h and the number of living bacteria decreased more than 99% after 8 h. In the cytotoxicity assay, during 48 h, Fe₃O₄NPs@RA had no cytotoxic effect on HEK-293 cells at concentrations lower than of 300 μg/ml. Conclusion: The results of the present study showed that Fe₃O₄NPs@RA were effective in inhibiting the growth and biofilm formation of S. aureus isolates and could be further investigated as an option for controlling S. aureus in food samples.

Key words: Biofilm, Magnetic nanoparticles, Rosmarinic acid, Staphylococcus aureus

Introduction

Foodborne pathogens are among the major causes of disease and death. The effects of foodborne pathogens on food safety and public health remain one of the most significant challenges in the health care systems around the world (Liang *et al.*, 2023).

Staphylococcus aureus is a successful, ubiquitous, opportunistic pathogen in humans and one of the common causes of food poisoning. It can grow in relatively low humidity and a wide range of temperatures, pH, and sodium chloride concentrations (Romano et al., 2023). S. aureus can colonize the skin and mucous membranes of approximately 30-60% of healthy people. It can also be found on the skin of animals, water, soil, and other surfaces which contaminate foods and makes them a possible source of human infection (Pal et al., 2022; Romano et al., 2023). Food preservatives have been used for centuries to

maintain food quality and control microbial growth. While synthetic food preservatives are convenient for processing, concerns over their safety persist. Consequently, there is a growing trend in the food industry to seek safe alternatives (Gyawali and Ibrahim, 2014; Park *et al.*, 2019).

One promising alternative is the use of medicinal plants with antimicrobial properties as food preservatives. Essential oils and plant extracts have been studied as important natural antimicrobial agents for years. Rosemary essential oil, in particular, is considered a natural food preservative due to its strong antimicrobial and antioxidant properties (Xie *et al.*, 2017). The essential oil of rosemary contains several compounds, including borneol, limonene, camphene, camphor, and phenolic acids, such as rosmarinic acid, caffeic acid, and chlorogenic acid (Tiwari *et al.*, 2005).

Rosmarinic acid (RA), an ester of caffeic acid with 3,4-dihydroxyphenyllactic acid is a phenolic compound

found in nature. RA has demonstrated significant biological effects, including: antiviral, antibacterial, anticancer, antioxidant, antiaging, antidiabetic, heart protective, liver protective, kidney protective, antidepressant, antiallergic and anti-inflammatory activity (Madureira et al., 2016). In terms of antimicrobial activity, RA has shown inhibitory effects against yeast and mold, Staphylococcus aureus, Enterobacteriaceae, Pseudomonas spp., lactic acid bacteria, Listeria monocytogenes and several other pathogenic bacteria. RA can disrupt bacterial cell structures and proteins, prevent biofilm development, inhibit quorum sensing, and display synergistic effects with various antibiotics, suggesting its potential as an effective antimicrobial agent (Nadeem et al., 2019; Kernou et al., 2023; Harindranath et al., 2024). However, its inadequate membrane permeability leads to reduced bioavailability and restricts its biological applications (Yang et al., 2018; Le et al., 2024). To enhance the bioavailability of RA, it has been incorporated with different nanoparticles including chitosan nanoparticles (da Silva et al., 2016), solid lipid nanoparticles (Madureira et al., 2016) and organo-silica nanoparticles (Le et al., 2024).

Magnetic nanoparticles, such as magnetite (Fe₃O₄) have garnered significant attention due to their small size, low toxicity, extensive surface area, and robust magnetic properties. The primary benefit they offer is their ability to be easily controlled and directed by a magnetic field, greatly facilitating the separation of different biomolecules (Cornell *et al.*, 2000; Laurent *et al.*, 2014). The present study aimed to incorporate RA in Fe₃O₄ nanoparticles (Fe₃O₄NPs) and investigate their effects on inhibiting the growth and biofilm formation of *S. aureus* isolated from poultry meat.

Materials and Methods

Synthesis of Fe₃O₄NPs@RA

Fe₃O₄NPs were purchased from Sigma-Aldrich (Germany). First, 1 g of Fe₃O₄NPs were dispersed in toluene (50 ml) using an ultrasound bath (15 min). Next, 2 ml of (3-chloropropyl) triethoxysilane was carefully introduced into the mixture and refluxed at 110°C for 1 h. The solution was then filtered and dried in an oven for 24 h. The obtained powder was collected from the filter paper. Subsequently, RA (0.3 g) was dissolved in 30 ml of DMSO. Fe₃O₄@(CH₂)₃Cl (0.15 g) nanoparticles and KI (0.17 g) were incorporated into the mixture, which was then agitated in an ultrasound bath for 2 h. Finally, the RA-loaded nanoparticles were filtered and dried in an oven at 50°C (Ghadimi *et al.*, 2025).

Confirmation of the synthesis of Fe₃O₄NPs@RA

The surface binding of RA to iron nanoparticles was confirmed by analyzing the product from the previous step using FT-IR (fourier transform infrared spectroscopy), XRD (X-ray diffraction), TEM, and VSM tests.

Tested bacteria

S. aureus was isolated from poultry meat samples and identified through biochemical tests, including its ability to grow on mannitol salt agar and the production of coagulase, catalase, DNase, and hemolysin enzymes (Romano *et al.*, 2023). Further characteristics of the test bacteria were investigated using the following tests.

Assessment of biofilm production ability in test bacteria

The biofilm-forming ability of the test isolates was evaluated using the microplate method. Standard overnight cultures $(1.5 \times 10^8 \text{ CFU/ml})$ of the test bacteria were diluted 100 times in Tryptic soy broth with 1% glucose. Staphylococcus epidermidis ATCC 12228 and Staphylococcus epidermidis ATCC 35984 strains served as negative and positive controls for assessing biofilm formation, respectively. Then, 200 μL from each culture dilution was added to separate wells of a 96-well flatbottomed polystyrene plate and incubated overnight at 37°C for 48 h. After that, the wells were rinsed 3 times with PBS to eliminate planktonic bacteria and then fixed with methanol for a duration of 20 min. Subsequently, each well received 200 µL of 0.02% crystal violet staining, rinsed with distilled water for 5 min, and the plates were dried. Biofilm formation was quantified by adding 200 µL of 33% glacial acetic acid to each well and measuring the optical density (OD) at 570 nm using an ELISA reader. The biofilm formation level was categorized as strong biofilm producer (OD >1.500), a biofilm producer (0.500 > OD > 1.500) or negative for biofilm production (OD <0.500) (Shafiei et al., 2014).

Investigating the antimicrobial effect of RA, Fe₃O₄NPs@Si (CH₂)₃Cl NPs and Fe₃O₄NPs@RA

To assess the antimicrobial impact of RA, Fe₃O₄NPs@Si (CH₂)₃Cl NPs, and Fe₃O₄NPs@RA on chosen *S. aureus* isolates, the minimum inhibitory concentration (MIC) was established using the broth microdilution technique. Serial concentrations of RA, Fe₃O₄NPs, and Fe₃O₄NPs@RA ranging from 2-4000 μ g/ml in 100 μ L of Mueller Hinton broth were created. Next, 100 μ L of the standardized overnight bacterial suspension (1.5 × 10⁶ CFU/ml) was introduced into each well, followed by incubation of the plates for 24 h at 37°C. This procedure was conducted three times.

Assessment of the combined antimicrobial effect of RA and $Fe_3O_4@Si(CH_2)_3Cl\ NPs$

The checkerboard method was used to evaluate the combined impact of RA and Fe₃O₄@Si(CH₂)₃Cl NPs on *S. aureus* strains. To begin, RA and Fe₃O₄@Si(CH₂)₃Cl NPs were diluted in Mueller Hinton broth, and 8 varying concentrations of each, ranging from 1/32 × MIC to 4 × MIC, were prepared in a 96-well microplate. Each row of wells contained the same level of RA concentration, while each column held an equal level of Fe₃O₄@Si(CH₂)₃Cl NPs. Each well had a total volume of 200 μ L, with 100 μ L of 5 × 10⁵ CFU/ml of bacterial

suspension, 50 μ L of RA, and 50 μ L of Fe₃O₄@Si(CH₂)₃Cl NPs. Additionally, several control wells were set up, including drug-free control, bacteria-free control, and single antibacterial agent MIC control. Following a 24-hour incubation at 37°C, the MIC values were recorded. Each experiment was conducted 3 times, and synergy was assessed using the fractional inhibitory concentrations index (FICI) as previously described (Scandorieiro *et al.*, 2022).

Anti-biofilm effect of RA, Fe₃O₄NPs@Si(CH₂)₃Cl NPs and Fe₃O₄NPs@RA

Quantitative anti-biofilm activity was assessed using the 96-well microplate method. This method mirrored the evaluation of biofilm production ability, except that the trypticase medium included a sub-MIC concentration of tested antimicrobials. A comparison of the optical absorption of the treatments and the control revealed the impact of RA, Fe₃O₄NPs@Si(CH₂)₃Cl NPs, and Fe₃O₄NPs@RA on inhibiting the biofilm formation (Martínez *et al.*, 2021). This experiment was repeated 3 times.

Time kill assay

The time-kill assay was used to assess the effectiveness of RA, Fe₃O₄NPs@Si(CH₂)₃Cl NPs, and Fe₃O₄NPs@RA against *S. aureus* isolates at various time intervals within 24 h. For this experiment, a bacterial suspension of 5 × 10⁵ CFU/ml was incubated overnight in a 96-well plate with adjusted Mueller Hinton broth, supplemented with MIC and 0.5 MIC concentrations of RA, Fe₃O₄NPs, and Fe₃O₄NPs@RA in separate wells. The plate was incubated at 37°C, and time points of 0, 2, 4, 8, and 24 h, samples were taken from each well, serially diluted (1:10) with PBS, and plated on Mueller-Hinton agar to determine cell viability. The results have been reported as Log10 CFU/ml. Time-kill experiment was performed in triplicate (Fahimirad *et al.*, 2017).

Investigating the effect of RA, Fe₃O₄NPs@Si(CH₂)₃Cl NPs and Fe₃O₄NPs@RA on the expression of *icaA* and *ica*D

The identification of the *ica*A and *ica*D genes in the test bacteria was verified through PCR analysis. Following this, RNA extraction was performed on the test isolates that had been exposed to sub-MIC concentrations of RA, Fe₃O₄NPs@Si(CH₂)₃Cl NPs, and Fe₃O₄NPs@RA, using the Cinagen RNA extraction kit. A bacterial culture without any antimicrobial substances

served as the control. Subsequently, cDNA was generated from the extracted RNA with the use of random hexamer primers. Real-time PCR was performed using the cDNA as a template and the *16S rRNA* gene was employed as the standard gene. The specific primers for analyzed genes are shown in Table 1. The reaction was carried out in a total volume of 20 μL , using the Genet Bio Q9210 kit (South Korea) according to the manufacturer's instructions. Gene expression change was calculated through $2^{-\Delta\Delta CT}$. This experiment was performed 3 times.

Cytotoxicity of Fe₃O₄NPs@RA

The activity of mitochondrial dehydrogenases in the normal HEK-293 cell line was assessed to determine the cytotoxicity of Fe₃O₄NPs@RA, using the MTT assay kit (Yekta Tajhiz, Iran). The cells were sourced from the cell bank of Pasteur Institute of Iran and cultured in DMEM medium supplemented with 10% fetal bovine serum, 2 mM L-glutamine, penicillin (100 U/ml), and streptomycin (100 $\mu g/ml$) at 37°C with 5% CO₂. Subsequently, suspensions of HEK-293 cells (1 \times 104 cells/wells) were seeded onto 96-well plates, and exposed to different concentrations (100-500 $\mu g/ml$) of Fe₃O₄NPs@RA.

After 24-48 h of incubation, 10 μ L of MTT dye was added to the wells, and the plates were left to incubate for an additional 4 h. The formazan crystals were then dissolved in DMSO, and the optical density was recorded at 570 nm using an ELISA reader (Ghadimi *et al.*, 2025). This experiment was repeated 3 times. The rate of cell survival was assessed using the following formula:

Cell survival rate: (absorbance of treated cells / absorbance of control cells) $\times\,100$

Statistical analysis

All experiments were conducted 3 times, and the data were assessed using SPSS 18. Statistical variations between the groups were evaluated using One-way ANOVA followed by Tukey's post hoc test. A P-value of less than 0.05 was considered to be statistically significant.

Results

Characterization of Fe₃O₄NPs@RA

The preparation steps of $Fe_3O_4NPs@RA$ are shown in Fig. 1. The RA immobilization on the surface of

Table 1: List of oligonucleotide primers used in this study

Primer	Sequences (5´-3´)	Annealin Tem.	Amplicon size (bp)	Reference	
icaA	F: GAGGTAAAGCCAACGCACTC R: CCTGTAACCGCACCAAGTTT	60	151	Marques et al. (2021)	
icaD	F: ACCCAACGCTAAAATCATCG R: GCGAAAATGCCCATAGTTTC	60	211		
16S rRNA	F: GGGACCCGCACAAGCGGTGG R: GGGTTGCGCTCGTTGCGGGA	60	191		

 Fe_3O_4 nanoparticles was performed by applying the layer-by-layer fabrication procedure. The Fe_3O_4 nanoparticles were first reacted with (3-chloropropyl) triethoxysilane to generate $Fe_3O_4NPs@Si(CH_2)_3Cl$ nanoparticles. Then, the rosmarinic acid was added to react with the $Fe_3O_4NPs@Si(CH_2)_3Cl$. Finally, the $Fe_3O_4NPs@RA$ was prepared.

Fig. 1: Schematic illustration of the Fe₃O₄NPs@RA

The binding of rosmarinic acid to the surface of Fe₃O₄ nanoparticles was confirmed by FT-IR analysis. to the FT-IR characterization of Fe₃O₄NPs@RA, the stretching vibrations of OH were observed at 3327 cm⁻¹. The C=O and C=C stretching vibrations were observed at 1645 cm⁻¹, 1575 cm⁻¹, and 1522 cm⁻¹, respectively. The C-O stretching vibration was observed at 1238 cm⁻¹. The Fe-O-Fe stretching vibrations were detected at 552 cm⁻¹ (Fig. 2C). The comparison between the FT-IR spectrum of rosmarinic acid (Fig. 2B), Fe₃O₄NPs@Si(CH₂)₃Cl nanoparticles (Fig. 2A), and Fe₃O₄@RA (Fig. 2C), prepared particles provided the evidence that rosmarinic acid is successfully attached to Fe₃O₄NPs@Si(CH₂)₃Cl nanoparticles.

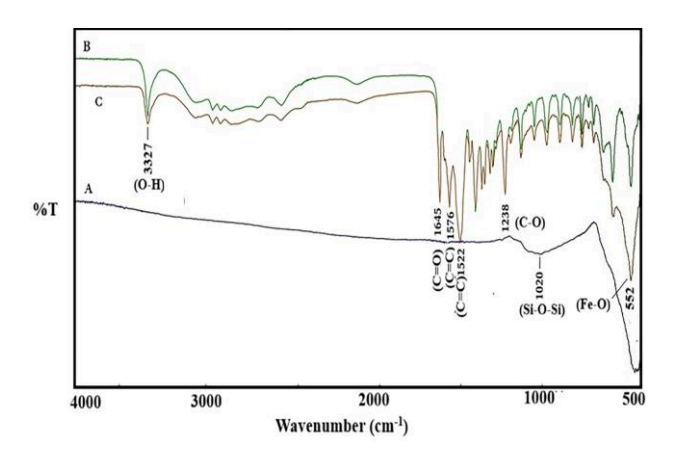


Fig. 2: FT-IR spectrum of (A) Fe₃O₄NPs@Si(CH₂)₃Cl, (B) rosmarinic acid, and (C) Fe₃O₄@RA nanoparticles

The XRD patterns of Fe₃O₄NPs@Si(CH₂)₃Cl, and Fe₃O₄NPs@RA nanoparticles are presented in Fig. 3. The XRD model of the Fe₃O₄NPs@RA demonstrated that the diffraction peaks were in match with the harmonic model of Fe₃O₄NPs. The XRD pattern of the Fe₃O₄NPs@RA nanoparticles shows six peaks at 30.24°, 35.59°, 43.24°, 53.84°, 57.29°, and 62.89°, related to (220), (311), (400), (422), (511) and (440) reflection planes of Fe₃O₄ (JCPDS NO.75-1609), respectively. These six typical peaks could be also found in the XRD patterns of the Fe₃O₄NPs@RA, indicating that the main crystal phase structure of Fe₃O₄NPs@Si(CH₂)₃Cl is maintained after rosmarinic acid conjugation. Also, the EDS spectrum shows the presence of C, O, Si and Fe elements in Fe₃O₄@RA (Fig. 4).

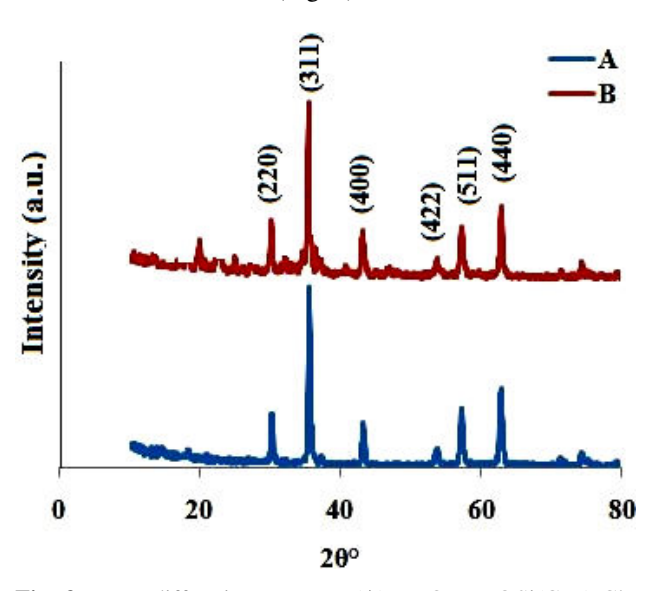


Fig. 3: XRD diffraction patterns. (A) Fe $_3$ O $_4$ NPs@Si(CH $_2$) $_3$ Cl, and (B) Fe $_3$ O $_4$ @RA nanoparticles

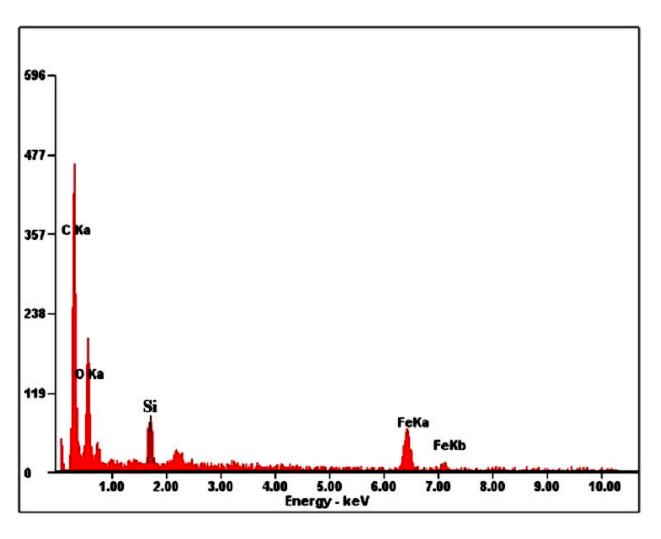
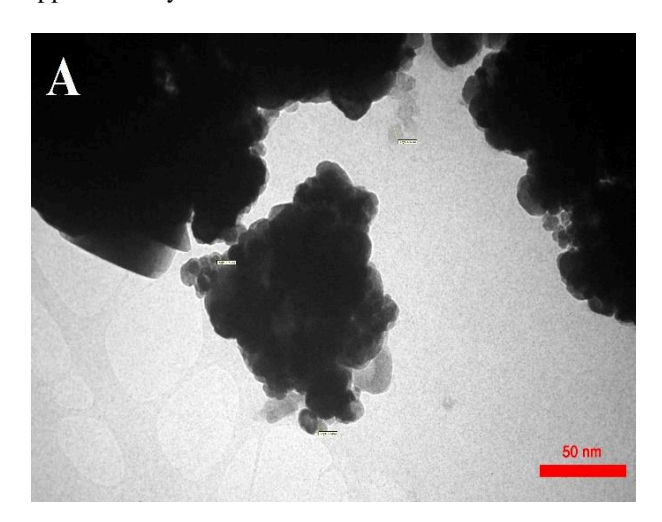


Fig. 4: EDX image of Fe₃O₄@RA NPs

The TEM micrograph of Fe $_3$ O $_4$ NPs@RA was investigated to study its particle topology, distribution and size. TEM image of Fe $_3$ O $_4$ NPs@RA shows a quasicube structure with low aggregation (Fig. 5A). According to the histogram diagram of the

Fe₃O₄NPs@RA (Fig. 5B) were observed at approximately 7-8 nm.



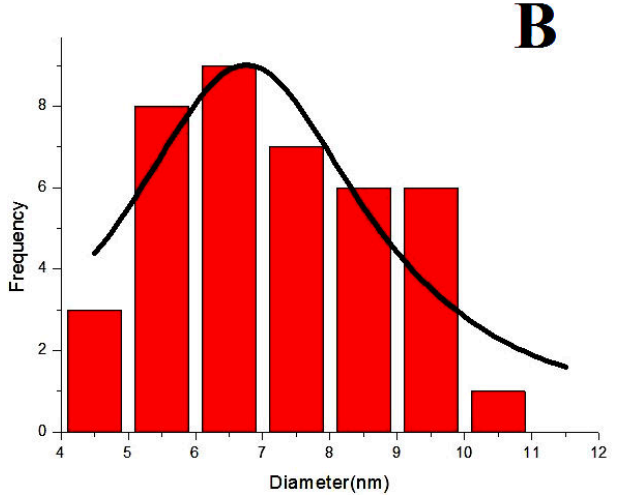


Fig. 5: (A) TEM image, and (B) histogram diagram of $Fe_3O_4NPs@RA$

The magnetic property of Fe $_3$ O $_4$ NPs@Si(CH $_2$) $_3$ Cl and Fe $_3$ O $_4$ @RA nanoparticles was evaluated by VSM at ambient temperature (Fig. 6). The saturation magnetization values of Fe $_3$ O $_4$ NPs@Si(CH $_2$) $_3$ Cl and Fe $_3$ O $_4$ @RA nanoparticles was 22.5 emu g $^{-1}$, 4.9 emu g $^{-1}$, respectively. When compared with the Fe $_3$ O $_4$ NPs@Si(CH $_2$) $_3$ Cl, the saturation magnetization of the Fe $_3$ O $_4$ @RA nanoparticles decreased due to the diamagnetic contribution of the thick SiO $_2$ and rosmarinic compounds.

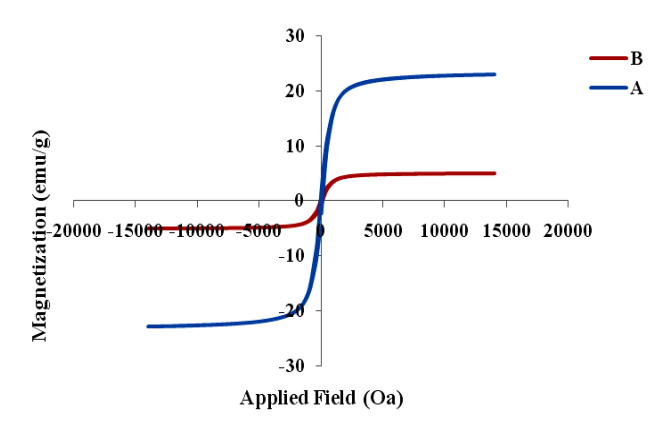


Fig. 6: VSM image of (A) Fe₃O₄NPs@Si(CH₂)₃Cl, and (B) Fe₃O₄NPs@RA

Table 2: MIC (μ g/ml) of RA, Fe₃O₄NPs@Si(CH₂)₃Cl NPs and Fe₃O₄NPs@RA in test bacteria

Test bacteria	MIC (μg/ml)				
	1	2	3	4	5
Fe ₃ O ₄ NPs@Si(CH ₂) ₃ Cl	1000	1000	1000	1000	1000
RA	1000	1000	1000	500	500
Fe ₃ O ₄ NPs@RA	125	62.5	62.5	31.2	31.2

Tested bacteria

In this study, Gram-positive cocci fermenting mannitol in mannitol salt agar medium with the ability to produce catalase, coagulase, DNase and hemolysin enzymes isolated from chicken meat food samples were identified as *S. aureus*. After phenotypic tests, 5 strong biofilm former isolates were selected for the study.

Antimicrobial effect of RA, Fe₃O₄NPs@Si(CH₂)₃Cl NPs and Fe₃O₄NPs@RA

The minimum inhibitory concentration (MIC) of Fe₃O₄NPs@Si(CH₂)₃Cl NPs against 5 *S. aureus* isolates was 1000 μ g/ml. This value varied between 500-1000 μ g/ml in the case of RA and between 31.2-125 μ g/ml in the case of Fe₃O₄NPs@RA (Table 2).

Combined activity of RA and Fe₃O₄@Si(CH₂)₃Cl NPs

The impact of the combined use of RA and Fe₃O₄@Si(CH₂)₃Cl nanoparticles on the proliferation of *S. aureus* isolates is presented in Table 3. RA and Fe₃O₄@Si(CH₂)₃Cl nanoparticles demonstrated synergistic and partially synergistic effects in four and one isolates, respectively.

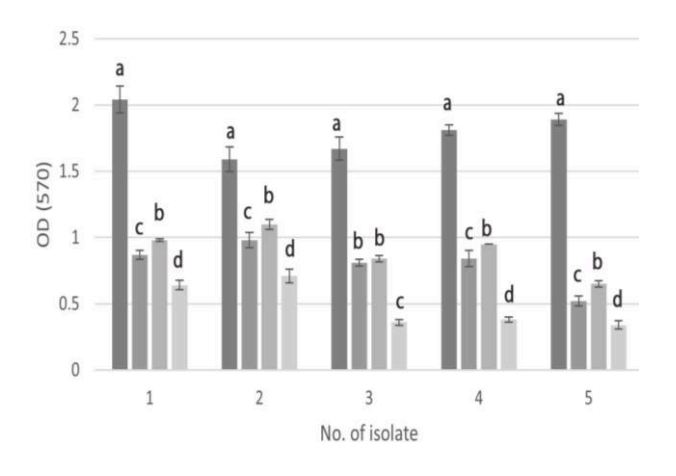
Table 3: The combined activity of RA and Fe₃O₄NPs@Si(CH₂)₃Cl against test bacteria

Bacterial No.	MIC _{alone} (µg/ml)		$MIC_{combined} \; (\mu g/ml)$		FICI value
	RA	Fe ₃ O ₄ NPs@Si(CH ₂) ₃ Cl	RA	Fe ₃ O ₄ NPs@Si(CH ₂) ₃ Cl	_
1	1000	1000	125	500	0.62
2	1000	1000	250	250	0.5
3	1000	1000	125	250	0.5
4	500	1000	62.5	250	0.37
5	500	1000	62.5	250	0.37

FICI \leq 0.5 indicates synergy, and 0.5 \leq FICI \leq 0.75 indicates partial synergy interactions

Anti-biofilm effect of RA, Fe₃O₄NPs@Si(CH₂)₃Cl and Fe₃O₄NPs@RA

Treatment of the *S. aureus* isolates with 1/2 MIC concentration of RA, Fe₃O₄NPs@Si(CH₂)₃Cl and Fe₃O₄NPs@RA led to a significant decrease in biofilm formation of the isolates. These compounds showed a reduction in the formation of biofilm up to 1/8 MIC concentration (OD<1.5). The range of biofilm inhibition in the conditions treated with the sub-MIC concentration of Fe₃O₄NPs@Si(CH₂)₃Cl in the 5 studied isolates was between 29 and 66%. The application of the sub-inhibitory concentration of RA resulted in inhibition of 37-78% and treatment with Fe₃O₄NPs@RA in different isolates inhibited biofilm formation by 50-82% (Fig. 7).



■ Control ■ RA ■ Fe₃O₄ NPs@Si(CH2)3Cl NPs ■ Fe₃O₄NPs@RA

Fig. 7: Optical absorption results of *S. aureus* isolates treated with 1/2 MIC concentration of the RA, Fe₃O₄NPs@Si(CH₂)₃Cl and Fe₃O₄NPs@RA compared to the control. Different letters on the columns indicate significant differences (P<0.05)

Time kill assay

The bactericidal activity of different concentrations of RA, Fe₃O₄NPs@Si(CH₂)₃Cl and Fe₃O₄NPs@RA against the selected isolate of S. aureus in terms of changes in log10 CFU/ml of living cells is shown in Fig. 8. In the control sample, the log CFU/ml reached 12.2 after 24 h of incubation at 37°C. Treatment with 1/2 MIC concentrations of RA, Fe₃O₄NPs@Si(CH₂)₃Cl, and Fe₃O₄NPs@RA resulted in a gradual decrease in the bacterial count between 0 and 24 h. Specifically, RA, Fe₃O₄NPs@Si(CH₂)₃Cl, and Fe₃O₄NPs@RA decreased the log CFU/ml by 3.4, 3, and 4.3, respectively (Fig. 8). At the MIC concentration of RA, a significant reduction in the S. aureus population was observed, with a 3-fold decrease in the bacterial count occurring after 8 h of exposure compared with the control population. Similarly, treatment with Fe₃O₄NPs@Si(CH₂)₃Cl at MIC concentration led to a gradual decrease in the bacterial population, with a 2.6-fold reduction after 8 h. Treatment with the MIC concentration of Fe₃O₄NPs@RA caused a 2.4-fold decrease in viable bacteria after 4 h, and after 8 h of exposure, the bacterial population was reduced to zero (Figs. 8-10).

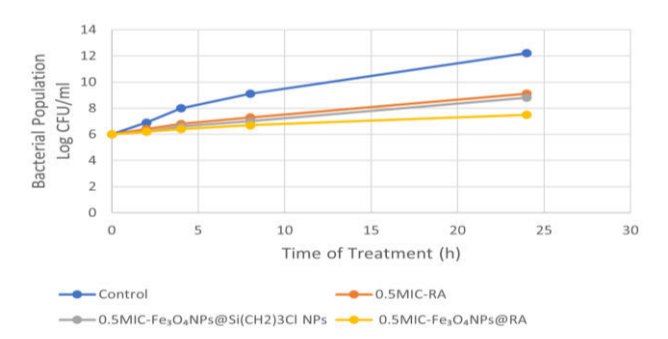


Fig. 8: The effect of 0.5 MIC concentration of RA, Fe₃O₄NPs@Si(CH₂)₃Cl and Fe₃O₄NPs@RA on the killing of *S. aureus* at different times

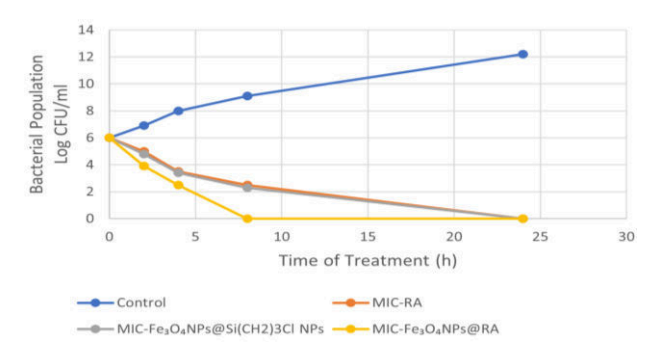


Fig. 9: The effect of MIC concentration of RA, Fe₃O₄NPs@Si(CH₂)₃Cl and Fe₃O₄NPs@RA on the killing of *S. aureus* at different times

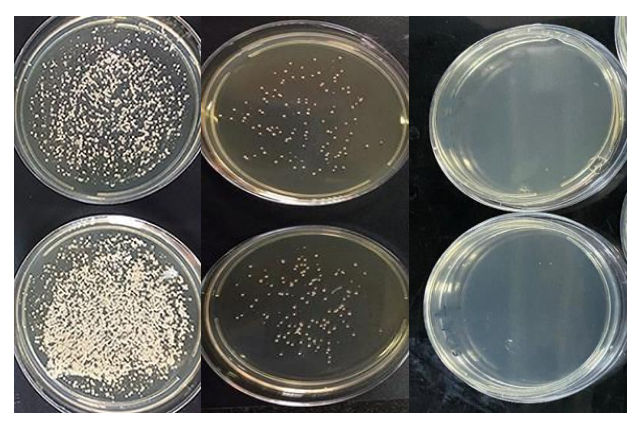


Fig. 10: Comparison of the bactericidal effect of Fe₃O₄NPs@RA at 2, 4 and 8 h of incubation (right to left)

Effect of Fe₃O₄NPs, RA and Fe₃O₄NPs@RA on the expression of *ica*A and *ica*D

The relative expression of *ica*A and *ica*D genes were assessed in *S. aureus* exposed to sub-MIC concentrations of Fe₃O₄NPs@Si(CH₂)₃Cl, RA, and Fe₃O₄NPs@RA, in comparison with untreated cells. These treatments led to a significant down-regulation of *ica*A and *ica*D genes (P<0.05), compared with housekeeping gene (*16S rRNA*, used as control) in all test bacteria. The level of expression of *ica*A and *ica*D was significantly reduced when exposed to sub-MIC concentrations of Fe₃O₄NPs@Si(CH₂)₃Cl, RA and Fe₃O₄NPs@RA in comparison with untreated cells. Moreover, when bacterial cells were exposed to sub-MIC concentrations

of Fe₃O₄NPs@RA, expression of *ica*A and *ica*D genes was reduced by over 60% in comparison with the control (Fig. 11).

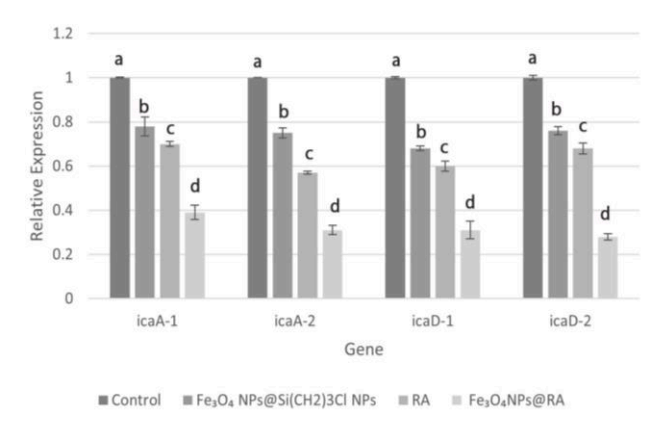


Fig. 11: Changes in the expression level of *ica*A and *ica*D genes in *S. aureus* isolates treated with sub-MIC concentration of Fe₃O₄NP₈@RA. Different letters on the columns indicate significant differences (P<0.05)

Cytotoxicity of Fe₃O₄NPs@RA

The cytotoxic effects of various concentrations of Fe₃O₄NPs@RA were assessed on HEK-293 cells using the MTT assay. The outcome was expressed as the percentage of cell viability for cultures containing five distinct concentrations (50, 100, 200, 300, 400, and 500 $\mu g/ml)$ of Fe₃O₄NPs@RA for 24. The viability of controls was set at 100%. The findings demonstrated that Fe₃O₄NPs@RA did not exhibit cytotoxic effects at concentrations below 400 $\mu g/ml$. More than 90% of the cells exposed to 400 $\mu g/ml$ Fe₃O₄NPs@RA for 24 h remained viable (P<0.05). After 48 h, Fe₃O₄NPs@RA showed no cytotoxic effects at concentrations below 300 $\mu g/ml$, with more than 85% of cells treated with 300 $\mu g/ml$ remaining viable (Fig. 12).

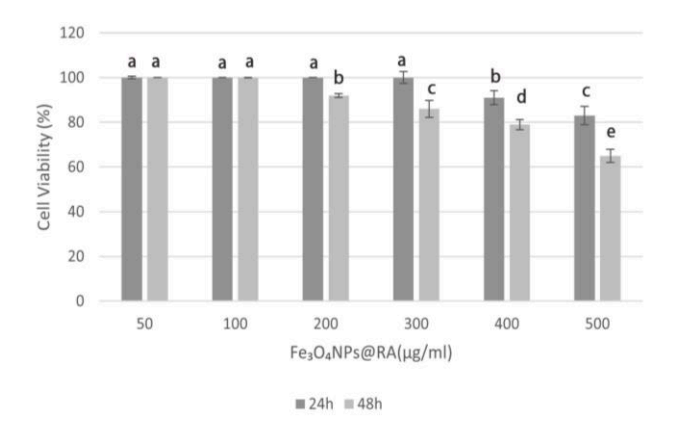


Fig. 12: Viability of HEK-293 cells in the presence of different concentrations of Fe₃O₄NPs@RA after 24 and 48 h. Different letters on the columns indicate significant differences (P<0.05)

Discussion

The use of herbal compounds to treat infections has a long-standing history in many parts of the world,

particularly in developed countries. Paying attention to medicinal plants that possess antimicrobial characteristics can solve frequent issues related to antibiotic usage. Plant essential oils have been recognized as important natural antimicrobial agents (Tiwari et al., 2005; Bakkali et al., 2008). These oils are of particular interest due to their broad-spectrum antimicrobial effects and potential as food additives (McKay et al., 2009). Rosemary essential oil contains compounds that have demonstrated antimicrobial and antioxidant properties in numerous studies, with phenolic antimicrobial compounds being particularly abundant in it (Wagnera and Ulrich-Merzenich, 2009). Rosmarinic acid is one of the most prevalent phenolic acids found in the Lamiaceae family (Petersen, 2013). Given the global significance of foodborne diseases, the present study investigated the antibacterial and antibiofilm effects of Fe₃O₄NPs@Si(CH₂)₃Cl, RA and Fe₃O₄NPs@RA against food-origin S. aureus isolates.

The results of our study revealed that RA exhibited inhibitory effect against S. aureus isolates with MIC values ranging between 500-1000 µg/ml. Loading RA onto Fe₃O₄NPs@Si(CH₂)₃Cl enhanced its antimicrobial activity improving the MIC values to 31.2-62.5 µg/ml. Antibacterial activity of RA has been shown against some pathogenic bacteria. Mencherini et al. (2007) identified the bacteriostatic properties of RA against Gram-positive bacteria, specifically S. aureus and S. epidermidis, while Klancnik et al. (2010) studied the antimicrobial efficacy of RA on Bacillus cereus, S. aureus, Salmonella infantis, Campylobacter jejuni, and C. coli reporting MIC values of 6 mg/ml, 10 mg/ml, 1.25 mg/ml, 1.25 mg/ml, and 1.25 mg/ml, respectively (Klancnik et al., 2010). Additionally, Slobodníková et al. (2013) observed MIC values of 625-1250 µg/ml against S. aureus, including MRSA strains. The low solubility and poor membrane permeability of RA are the primary reasons for its poor bioavailability (Le et al., 2024). To address these limitations, previous studies have explored enhancing the bioavailability of RA by infusing it into nanoparticles, including chitosan nanoparticles (da Silva et al., 2016), solid lipid nanoparticles (Madureira et al., 2016), phospholipid complexes (Huang et al., 2019), or cyclodextrins (Aksamija et al., 2016). In the present study, RA was successfully loaded onto Fe₃O₄NPs, and the antimicrobial, antibiofilm, and bactericidal properties of free and loaded RA were compared. The results Fe₃O₄NPs@RA showed that the formulation significantly enhanced antimicrobial activity, improving MIC values 8-10 times as compared with free RA. In the time-kill assay, treatment with Fe₃O₄NPs@RA at MIC concentration resulted in a 2.4-fold decrease in bacterial population after 4 h, with complete elimination of viable bacteria by 8 h.

S. aureus is a major pathogen known for its ability to form biofilms, which protect bacteria from external threats, including antimicrobial agents (Wang et al., 2025). The minimum concentrations of many antibiotics needed to eliminate biofilms are often much greater than the MIC measured in their planktonic state, which limits

their effectiveness in treating biofilm-associated infections (Kotulova and Slobodnikova, 2010). Given that biofilms are responsible for approximately 80% of bacterial infections, there is a critical need for new antimicrobial agents effective against both planktonic forms and biofilm growth of bacteria (Rama et al., 2016). Previous research has demonstrated that RA is effective in reducing biofilm formation and disrupting planktonic cell activity (Raeisi et al., 2016). RA has also been reported to inhibit quorum sensing and biofilm formation in Aeromonas hydrophila strains (Ivanov et al., 2022). Therefore, this study aimed to investigate RA activity in the biofilm formation of S. aureus strains isolated from food. Our results show that treatment of the S. aureus isolates with 1/2 MIC concentration of RA, Fe₃O₄NPs, and Fe₃O₄NPs@RA led to a significant decrease in biofilm formation. With the strongest antibiofilm effect, treatment with a sub-inhibitory concentration of Fe₃O₄NPs@RA prevented biofilm formation in different isolates by 50 and 82%, and a significant reduction in the expression of icaA and icaD genes (associated with biofilm formation) was observed, with a decrease of more than 60% as compared with control samples. These findings suggest that Fe₃O₄NPs@RA has the potential to inhibit biofilm formation in the tested *S. aureus* isolates.

The development of non-toxic antibacterial and antibiofilm agents has garnered significant attention in pharmaceutical research (Paseban et al., 2024). However, the potential cytotoxicity of nanoparticles, including Fe₃O₄NPs, has limited their biological applications. To mitigate this concern, researchers have explored surface modification with natural compounds to reduce cytotoxicity (Al-Hunaiti et al., 2024). In this study, the cytotoxicity of Fe₃O₄NPs@RA was assessed on HEK-293 cells using the MTT assay. The results indicated that Fe₃O₄NPs@RA did not exhibit cytotoxic effects on cell viability at concentrations lower than 400 μg/ml for 24 h and 300 μg/ml for 48 h. This finding is consistent with a recent study by Al-Hunaiti et al. (2024). They showed that RA-loaded nanoparticles exhibited lower cytotoxicity compared to unmodified magnetic nanoparticles, potentially offering protection against normal cell toxicity. Although, Fe₃O₄NPs@RA appears to be safe at low concentrations, the biosafety of this nanoparticle requires more attention. Further in vitro and in vivo studies are needed to fully understand its long-term biosafety profiles and interaction with biological systems.

The results of this study demonstrate that Fe₃O₄NPs@RA effectively inhibits the growth and biofilm formation of *S. aureus* isolates. This formulation shows promise as a potential strategy for controlling *S. aureus* in food samples, offering both antimicrobial and antibiofilm properties with minimal cytotoxicity to mammalian cells. Further studies are warranted to explore its application in real-world scenarios and its safety profile in biological systems.

Acknowledgement

The authors would like to thank the Islamic Azad University, Rasht Branch, Rasht, Iran, for their support.

Conflict of interest

The authors declare that there is no conflict of interest.

References

- Aksamija, A; Polidori, A; Plasson, R; Dangles, O and Tomao, V (2016). The inclusion complex of rosmarinic acid into beta-cyclodextrin: A thermodynamic and structural analysis by NMR and capillary electrophoresis. Food Chem., 208: 258-263.
- Al-Hunaiti, A; Zihlif, M; Abu Thiab, T; Al-Awaida, W; Al-Ameer, HJ and Imraish, A (2024). Magnetic nanoparticle-based combination therapy: Synthesis and *in vitro* proof of concept of CrFe₂O₄-rosmarinic acid nanoparticles for anti-inflammatory and antioxidant therapy. PLoS One. 19: e0297716.
- Bakkali, F; Averbeck, S; Averbeck, D and Idaomar, M (2008). Biological effects of essential oils - a review. Food Chem. Toxicol., 46: 446-475.
- Cornell, RM and Schwertmann, U (2000). The iron oxides: structure, properties, reactions, occurrences and uses. 2nd Edn., Darmstadt, Germany, Wiley. PP: 1-8.
- da Silva, SB; Ferreira, D; Pintado, M and Sarmento, B (2016). Chitosan-based nanoparticles for rosmarinic acid ocular delivery—in vitro tests. Int. J. Biol. Macromol., 84: 112-120.
- Fahimirad, S; Abtahi, H; Razavi, SH; Alizadeh, H and Ghorbanpour, M (2017). Production of recombinant antimicrobial polymeric protein beta casein-E 50-52 and its antimicrobial synergistic effects assessment with thymol. Molecules. 22: 822-838.
- Ghadimi, N; Asadpour, L and Mokhtary, M (2025). Enhanced antimicrobial, anti-biofilm, and efflux pump inhibitory effects of ursolic acid-conjugated magnetic nanoparticles against clinical isolates of multidrug-resistant Pseudomonas aeruginosa. Microb. Pathog., 199: 107241-107250.
- **Gyawali, R and Ibrahim, SA** (2014). Natural products as antimicrobial agents. Food Control. 46: 412-429.
- Harindranath, H; Susil, A; Rajeshwari, S; Sekar, M and Kumar, BP (2024). Unlocking the potential of rosmarinic acid: A review on extraction, isolation, quantification, pharmacokinetics and pharmacology. Phytomed. Plus., 29: 100726-100746.
- **Huang, J; Chen, PX; Rogers, MA and Wettig, SD** (2019). Investigating the phospholipid effect on the bioaccessibility of rosmarinic acid-phospholipid complex through a dynamic gastrointestinal *in vitro* model. Pharmaceutics. 11: 156-174.
- Ivanov, M; Kostić, M; Stojković, D and Soković, M (2022).
 Rosmarinic acid-modes of antimicrobial and antibiofilm activities of a common plant polyphenol. S. Afr. J. Bot., 146: 521-527.
- Kernou, ON; Azzouz, Z; Madani, K and Rijo, P (2023).
 Application of rosmarinic acid with its derivatives in the treatment of microbial pathogens. Molecules. 28: 4243-4263.

- Klancnik, A; Piskernik, S; Jersek, B and Smole Mozina, S (2010). Evaluation of diffusion and dilution methods to determine the antibacterial activity of plant extracts. J. Microbiol. Methods. 81: 121-126.
- **Kotulova, D and Slobodnikova, L** (2010). Susceptibility of *Staphylococcus aureus* biofilms to vancomycin, gentamicin and rifampin. Epidemiol. Microbiol. Immunol., 59: 80-87.
- Laurent, S; Saei, AA; Behzadi, S; Panahifar, A and Mahmoudi, M (2014). Superparamagnetic iron oxide nanoparticles for delivery of therapeutic agents: opportunities and challenges. Expert Opin. Drug Deliv., 11: 1449-1470.
- Le, UC; Mai, NX; Le, KM; Vu, HA; Tran, HN and Doan, TL (2024). Development and evaluation of rosmarinic acid loaded novel fluorescent porous organosilica nanoparticles as potential drug delivery system for cancer treatment. Arab. J. Chem., 17: 105402-105411.
- Liang, T; Liang, Z; Wu, S; Ding, Y; Wu, Q and Gu, B (2023). Global prevalence of *Staphylococcus aureus* in food products and its relationship with the occurrence and development of diabetes mellitus. Med. Adv., 1: 53-78.
- Madureira, AR; Campos, DA; Oliveira, A; Sarmento, B; Pintado, MM and Gomes, AM (2016). Insights into the protective role of solid lipid nanoparticles on rosmarinic acid bioactivity during exposure to simulated gastrointestinal conditions. Colloids Surf. B., 139: 277-284.
- Marques, VF; Santos, HA; Santos, TH; Melo, DA; Coelho, SM; Coelho, IS and Souza, M (2021). Expression of *ica*A and *ica*D genes in biofilm formation in *Staphylococcus aureus* isolates from bovine subclinical mastitis. Pesq. Vet. Bras., 41: e06645.
- Martínez, A; Manrique-Moreno, M; Klaiss-Luna, MC; Stashenko, E; Zafra, G and Ortiz, C (2021). Effect of essential oils on growth inhibition, biofilm formation and membrane integrity of *Escherichia coli* and *Staphylococcus aureus*. Antibiotics. 10: 1474-1489.
- McKay, GA; Beaulieu, S; Arhin, FF; Belley, A; Sarmiento, I; Parr, JrT and Moeck, G (2009). Time-kill kinetics of oritavancin and comparator agents against *Staphylococcus aureus*, *Enterococcus faecalis* and *Enterococcus faecium*. J. Antimicrob. Chemother., 63: 1191-1199.
- Mencherini, T; Picerno, P; Scesa, C and Aquino, R (2007). Triterpene, antioxidant, and antimicrobial compounds from *Melissa officinalis*. J. Nat. Prod., 70: 1889-1894.
- Nadeem, M; Imran, M; Aslam Gondal, T; Imran, A; Shahbaz, M; Muhammad Amir, R; Wasim Sajid, M; Batool Qaisrani, T; Atif, M; Hussain, G and Salehi, B (2019). Therapeutic potential of rosmarinic acid: A comprehensive review. J. Appl. Sci., 9: 3139-3161.
- Pal, M; Ketchakmadze, D; Durglishvili, N and Ketchakmadze, K (2022). Staphylococcus aureus: A major pathogen of food poisoning: A rare research report. Nutr. Food Process., 5: 1-3.
- **Park, J; Rho, SJ and Kim, YR** (2019). Enhancing antioxidant and antimicrobial activity of carnosic acid in rosemary (*Rosmarinus officinalis* L.) extract by complexation with cyclic glucans. Food Chem., 299: 125119-125129.
- Paseban, K; Noroozi, S; Gharehcheloo, R; Haddadian, A;

- Robattorki, FF; Dibah, H; Amani, R; Sabouri, F; Ghanbarzadeh, E; Hajrasouiha, S and Azari, A (2024). Preparation and optimization of niosome encapsulated meropenem for significant antibacterial and anti-biofilm activity against methicillin-resistant *Staphylococcus aureus* isolates. Heliyon. 10: e35651.
- **Petersen, M** (2013). Rosmarinic acid: new aspects. Phytochem. Rev., 12: 207-227.
- Raeisi, M; Tabaraei, A; Hashemi, M and Behnampour, N (2016). Effect of sodium alginate coating incorporated with nisin, Cinnamomum zeylanicum, and rosemary essential oils on microbial quality of chicken meat and fate of Listeria monocytogenes during refrigeration. Int. J. Food Microbiol., 238: 139-145.
- Rama Devi, K; Srinivasan, R; Kannappan, A; Santhakumari, S; Bhuvaneswari, M; Rajasekar, P; Prabhu, NM and Veera Ravi, A (2016). *In vitro* and *in vivo* efficacy of rosmarinic acid on quorum sensing mediated biofilm formation and virulence factor production in *Aeromonas hydrophila*. Biofouling. 32: 1171-1183.
- Romano, A; Carrella, S; Rezza, S; Nia, Y; Hennekinne, JA; Bianchi, DM; Martucci, F; Zuccon, F; Gulino, M; Di Mari, C and Zaccaria, T (2023). First report of food poisoning due to staphylococcal enterotoxin type B in Döner Kebab (Italy). Pathogens. 12: 1139-1150.
- Scandorieiro, S; Rodrigues, BC; Nishio, EK; Panagio, LA; De Oliveira, AG; Durán, N; Nakazato, G and Kobayashi, RK (2022). Biogenic silver nanoparticles strategically combined with *Origanum vulgare* derivatives: Antibacterial mechanism of action and effect on multidrugresistant strains. Front. Microbiol., 13: 842600-84626.
- Shafiei, M; Ali, AA; Shahcheraghi, F; Saboora, A and Noghabi, KA (2014). Eradication of *Pseudomonas aeruginosa* biofilms using the combination of n-butanolic cyclamen coum extract and ciprofloxacin. Jundishapur J. Microbiol., 7: e14358.
- Slobodníková, L; Fialová, S; Hupková, H and Grančai, D (2013). Rosmarinic acid interaction with planktonic and biofilm *Staphylococcus aureus*. Nat. Prod. Commun., 8: 1747-1750.
- **Tiwari, RP; Bharti, SK; Kaur, HD; Dikshit, R and Hoondal, GS** (2005). Synergistic antimicrobial activity of tea and antibiotics. Indian J. Med. Res., 122: 180-186.
- Wagnera, H and Ulrich-Merzenich, G (2009). Synergy research: Approaching a new generation of phytopharmaceuticals. Phytomedicine. 16: 97-110.
- Wang, D; Wang, L; Liu, Q and Zhao, Y (2025). Virulence factors in biofilm formation and therapeutic strategies for *Staphylococcus aureus*: A review. Anim. Zoonoses., 1: 188-202.
- Xie, J; VanAlstyne, P; Uhlir, A and Yang, X (2017). A review on rosemary as a natural antioxidation solution. Eur. J. Lipid Sci. Technol., 119: 1600439.
- Yang, JH; Mao, KJ; Huang, P; Ye, YJ; Guo, HS and Cai, BC (2018). Effect of piperine on the bioavailability and pharmacokinetics of rosmarinic acid in rat plasma using UPLC-MS/MS. Xenobiotica. 48: 178-185.